Comparison of Trajectory Tracking Controllers for Autonomous Vehicles

Davide Calzolari, Bastian Schürmann, and Matthias Althoff

***Abstract*—Controlling autonomous vehicles typically has two main components: planning a trajectory and tracking this trajectory using feedback controllers. To benefit from the recent progress in planning algorithms, it is key that the underlying tracking controller is able to follow the planned trajectory as desired. In emergency situations in particular, it is crucial that feedback controllers steer the vehicle as close as possible to the planned trajectory to remain within a safe corridor. While there exists much work on the design of trajectory and path tracking controllers for vehicles, little work has been done to systematically compare different approaches, especially when considering extreme situations, uncertain parameters, and disturbances. In this work, we compare eight tracking controllers in a systematic way, each of them representing a different controller family. By not only considering nominal behavior, but also sensor noise and uncertain parameters, we obtain for the first time a broad comparison of the behavior of different controllers in various situations.**

I. Introduction

Automated control of vehicles is a challenging task due to the non-linearity of the dynamics, the influence of sensor noise, disturbances, and unknown parameters, as well as due to safety criticality. Most control schemes are tracking maneuvers generated by high-level planners.

While closely tracking the planned trajectory is important in all driving situations, it becomes especially crucial when considering extreme maneuvers in emergency situations. Only if the tracking controller is able to control the car despite all previously mentioned disturbances is it possible to execute safe emergency maneuvers.

Since vehicle control is an important topic, many different methods and control algorithms for this problem have been developed. Control methods include sliding mode control [1], [2], [3], flatness-based control [4], [5], optimal linear-quadratic control [6], backstepping-based strategies [7], [8], [9], optimal preview control [10] and optimization-based methods like model predictive control (MPC) [11], [12].

Choosing the appropriate controller is a non-trivial task since control performance changes significantly depending on the scenario. To better guide the selection of the controller, we compare the tracking performance of different controllers.

In the last decades, several attempts have been made at comparing vehicle control performance: an example of comparing H_∞, adaptive, fuzzy and PID controllers can be found in [13]; of robust controllers in [14]; of predictive and LQ methods in [15]; of linear LQ and sliding mode in [16]; and of various kinematic-based algorithms in [17].

However, these comparisons do not consider the average and worst-case tracking performance of the controllers under sensor noise or other kinds of disturbances, which is extremely useful information when the system must provide safety guarantees.

Therefore, the authors in [5] developed a framework for systematically comparing the performance of controllers for vehicle trajectory tracking. While they presented a general framework, which considers various scenarios including the effects of sensor noise and model mismatch, they only compare two flatness-based controllers. Since those are quite similar, the comparison has been rather incomplete. Therefore, the goal of our paper is to build on the developed test scenarios from [5] and use it to compare a wide variety of different control schemes. This allows a control engineer to better judge which controller type works best in the considered situations.

The article is organized as follows: In Section II, the vehicle model employed for the comparison is described and all considered controllers are briefly introduced. The comparison framework from [5] is described in Section III. Section IV presents the tests results and the analysis for each test. Our conclusions are presented in Section V.

II. Model and Controllers

This section introduces the model used for our comparisons. We use the same single track model as in [5], which is a six-dimensional, non-linear vehicle model including a non-linear tire function to faithfully consider the tire/road interaction. Since we focus on emergency maneuvers, we limit our analysis to trajectories that eventually bring the vehicle to a safe standstill. The model assumes the front steering angle position and the front angular wheel speed as inputs. The steering angle is limited to $\pm 45°$. The tire force model is based on an approach similar to Pacejkas' one, using the normalized slip direction. This formulation provides a realistic approximation of the vehicle behavior considering tire forces saturation.

In the following paragraphs, eight controllers for vehicle tracking are briefly introduced, each based on a different control concept and based on different assumptions. These controllers do not cover the entire range of available feedback methods developed in the last decades, yet they are significant representatives of popular control concepts like flatness-based

This work has been financially supported by the European Commission project UnCoVerCPS under grant number 643921.

The authors are with the Department of Informatics, Technische Universität München, Boltzmannstr. 3, 85748 Garching, Germany (e-mail: {davide.calzolari, bastian.schuermann, althoff}@tum.de)

control, sliding mode control, passivity-based control, linear quadratic optimal control, and combined non-linear strategies. Note that we do not consider any controller which involves online optimization, including MPC controllers. In this case, the control performance directly depends on the optimization horizon and the used optimization algorithms, which makes a fair comparison very challenging. Because of these reasons, only algebraic and continuous time, feedback-based controllers are considered in this work.

A. Kinematic I/O Linearization (KINIO)

The design of trajectory-tracking controllers for non-holonomic vehicles is often based on input/output linearization via error feedback plus feed-forward action. This method is presented in [18] for the unicycle model. Using the same approach, a controller for the kinematic bicycle model was derived to track accelerations along the x and y axes. The orientation of the vehicle is not controlled.

B. Kinematic Sliding Mode (KINSM)

A control strategy robust against various kinds of disturbances is that of sliding mode. In [3] a sliding-mode controller for the tracking problem is described. The vehicle model is simplified to the kinematic non-holonomic system. The article presents a trajectory tracking controller with the control point at the rear tire and a path tracking controller with look-ahead control point. Herein, the former is considered for the comparison. As the authors point out, in this problem there are three variables to be controlled and only two inputs. Therefore the lateral and orientation errors have been coupled by one sliding surface in order to achieve convergence of both variables.

C. Higher-Order Sliding Mode (HOSM)

Higher order sliding mode control is useful to robustly track a reference trajectory while also reducing chattering. An example of this technique applied to vehicle control is presented in [14]. The *switching* part of the control is calculated by applying the Super-Twisting Theorem [14].

D. Immersion and Invariance (I&I)

In [14], a framework for trajectory tracking and stabilization of non-linear systems has been developed on the basis of the Immersion and Invariance Principle (I&I). The objective of I&I control is to immerse the dynamics of the plant into a target system with the desired behavior by defining an attractive and invariant manifold in the state-space. The control law can be interpreted as the simultaneous action of a dynamic state feedback controller, which compensates lateral and yaw dynamics, plus a PID controller, which rejects some disturbances and adjusts gains depending on the system parameters.

E. Passivity-based PI (PBPI)

Some interesting input-output passive mappings can be found by studying the intrinsic characteristics of vehicle dynamics. These mappings allow the design of passivity-based controllers, which can be useful in order to improve the robustness of an uncertain non-linear system. Since the performance of PI controller degrades when non-linearities play a major role in the dynamics, the authors of [14] present a passivity-based controller with an adaptive non-linear gain. The gain rapidly increases when the system needs large corrections and vanishes in the neighborhood of the desired state in order to prevent oscillations.

F. Flatness-based Approach (FLAT)

The differential flatness property can be exploited to derive a controller for a non-linear dynamic bicycle model. In [5] a comparison of two controllers that exploit the front and the rear decoupling points of the vehicle is presented. For our comparison, controller A (with front decoupling point) from [5] is used, since it performs sightly better in the considered scenarios than the one with rear decoupling point.

G. Infinite Horizon LQ Control (LQR)

Classical optimal control methods, like infinite time horizon LQR, are applied in [19]. For a particular velocity, the system is modeled as a linear system whose dynamic matrix is adjusted for each new velocity reading. Optimal gains are calculated offline for a range of operating speeds and linearly interpolated during the online phase. In order to improve tracking, a feed-forward steady-state term is added to the optimal steering angle.

H. Non-linear Backstepping Control (BKST)

A coordinated steering and braking control system based on the non-linear backstepping control theory has been developed in [7] in order to guarantee global asymptotic stability of controlled systems. As is the case for the other controllers with switching functions (KINSM and HOSM), the switching part of the control is approximated by a standard smooth function (tanh). A position error term is added to the longitudinal error in order to assure tracking at position and velocity level. The fuzzy adaptive version presented in the [7] is not used here.

I. Necessary Adjustments

Many approaches considered in this work for trajectory tracking have originally been developed for path tracking. In this work, we consider trajectory tracking since it allows us to specify the desired state at each point in time rather than demanding only to follow a path, which is crucial for emergency situations. Figure 1 illustrates the distinction between trajectory tracking errors and path following errors. Most trajectory tracking controllers define the tracking error as the difference between the desired state $\boldsymbol{x}_d(t)$ and the actual state $\boldsymbol{x}$ expressed in local vehicle-fixed coordinates. With Ψ as the orientation of the vehicle and $\boldsymbol{t}_v$, $\boldsymbol{n}_v$ the unit vectors of the x and y axes of the local coordinates

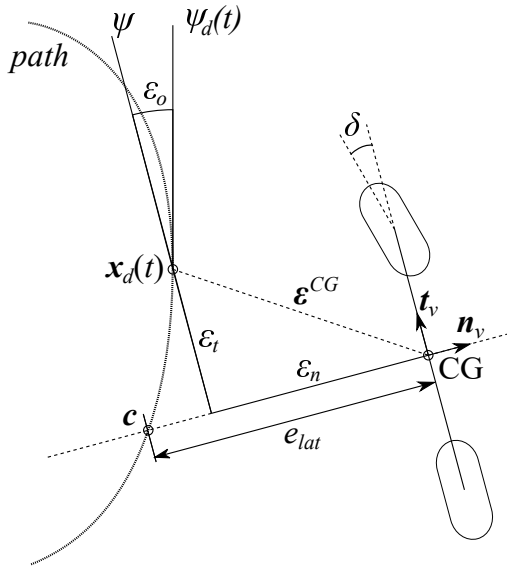

Fig. 1. Definition of tracking and path following errors

system, respectively, we focus on a subset of variables in $\boldsymbol{x}$ to define $\boldsymbol{\varepsilon}^{CP} = [\varepsilon_t, \varepsilon_n, \varepsilon_o]^T$, where $\varepsilon_t = (\boldsymbol{\varepsilon}^{CP})^T \boldsymbol{t}_v$, $\varepsilon_n = (\boldsymbol{\varepsilon}^{CP})^T \boldsymbol{n}_v$, $\varepsilon_o = \Psi_d - \Psi$ and CP indicates the control point.

The feedback error vector used by KINIO and FLAT controllers refers to a look-ahead point as described in [5]. Controllers HOSM, I&I, PBPI and LQR are lateral controllers and make use of vehicle path coordinates, which express lateral deviation (aka path following error) as $e_{lat} = \|\boldsymbol{CG} - \boldsymbol{c}\|$, where $\boldsymbol{CG}$ is the center of mass and $\boldsymbol{c}$ corresponds to the intersection between the path and the normal to the vehicle in driving direction (see Fig. 1). The BKST controller defines the lateral error as the shortest distance from a look-ahead point to the path.

To use all previously presented controllers for trajectory tracking, the deviation $\boldsymbol{\varepsilon}^{CG}$ is used for HOSM, I&I, PBPI, and LQR controllers, since they control the position of the CG, while the deviation $\boldsymbol{\varepsilon}^{D_L}$ is used for the BKST controller because it controls a look-ahead point at distance D_L from the CG. This slightly modifies the original control concepts, but since both orientation and tangential errors remain small, the normal tracking error ε_n approximates the path lateral deviation e_{lat}:

$$\text{if } \varepsilon_t \to 0 \text{ and } \varepsilon_o \to 0 \Rightarrow \boldsymbol{c} \approx \boldsymbol{x}_d \Rightarrow \varepsilon_n \approx e_{lat}.$$

Controllers HOSM, I&I, PBPI and LQR calculate only the steering angle to minimize the lateral deviation and do not control vehicle speed. Additionally, a longitudinal controller is needed for trajectory tracking. A PD controller is therefore used to track the required speed (parameters in Table I).

Different controllers often assume their own set of controllable inputs based on their specific model of the vehicle. In order to evaluate all the controllers using the same model, we map the inputs obtained by the different controllers to those required by the model. A description of the mappings,

TABLE I
PARAMETERS OF THE CONTROLLERS

Controller	Gains
KINIO*	$D_L = \frac{J}{ml_R}, K_p = 20, K_d = 20$
KINSM	$k_0 = 0.05, k_1 = 0.25, k_2 = 0.5,$ $p_1 = 1, p_2^* = 3, q_1 = 1, q_2^* = 3$
HOSM	$\lambda = 8, \alpha = 0.008, \beta = 0.008$
I&I	$\lambda = 8, K_1 = 2, K_2 = 0.5$
PBPI	$\lambda^* = 1, K_P^* = 0.075, K_I = 0.015,$ $e_{max} = 0.25, k_0 = 12$
FLAT	$\lambda = \frac{J}{ml_R}, K_p = 5, K_d = 3.3541$
LQR	$Q = diag([0.075, 0, 0, 0]), R = 1,$ K_{opt} calculated for $v_x \in$ [15, 22] m/s, in steps of 1 m/s
BKST*	$D_L = \frac{J}{ml_R}, \lambda_1 = 0.1, \lambda_2 = 0.1, k_1 = 10, k_2 = 1,$ $l_1 = 10, \gamma = 0, \zeta_1 = 1, \beta = 0, \epsilon_1 = 1$
PD	$P = 5, D = 5$, feedforward $a_{x,ref}$. Used by HOSM, I&I, PBPI and LQR.

the code for the controllers and comparison, and further details regarding modifications of original control concepts are available online at: https://bitbucket.org/MatthiasAlthoff/itsc2017_davidecalzolari.git.

Each controller has its own set of gains and a different number of available degrees of freedom. Correct tuning is important for a fair comparison and in order to highlight the intrinsic properties of each controller. Table I presents the gains that are used throughout all simulations. Wherever possible, the gains suggested by the authors are used. An asterisk (*) after the name of a controller means that the gains are not given in the corresponding article or book and are therefore manually set. Instead, an asterisk after a gain means that the value is sightly adjusted from the suggested value. The adjustments are only conducted when our parameters provide better results in our tests.

III. FRAMEWORK FOR COMPARISON

We use the same two typical emergency maneuvers presented in [5]: single and double lane change. The initial velocity of the double lane change trajectory has been reduced from 22 m/s to 21 m/s since most controllers cannot handle full tire saturation so that the deviation from the reference trajectory would become very large otherwise. Different tests are carried out on the scenarios in order to evaluate control robustness against initial deviations, measurement noise, tire saturation, and parameter uncertainties. Average and worst-case performance are evaluated using of Monte Carlo simulations and Rapid Exploring Random Trees (RRTs). By testing the aforementioned, diverse aspects, we can identify for which purpose the suggested controllers are most suitable.

A. Methodology

The tracking error (or deviation) is calculated as the distance between the car's center of mass and the reference $\boldsymbol{x}_d(t)$, expressed in local vehicle coordinates. The tangential and normal components of the deviation $\boldsymbol{\varepsilon}^{CG}_{\{t,n\}}$ are employed for the computation of different tracking performance measures:

$$\begin{aligned}
\text{maximum deviation:} \quad & \max_{t\in[0,T]} |\boldsymbol{\varepsilon}^{CG}_{\{t,n\}}(t)| \\
\text{average deviation:} \quad & \frac{1}{T}\int_0^T |\boldsymbol{\varepsilon}^{CG}_{\{t,n\}}(t)|dt \\
\text{final deviation:} \quad & \boldsymbol{\varepsilon}^{CG}_{\{t,n\}}(T) \\
\text{average tire saturation:} \quad & \frac{1}{T}\int_0^T \|\boldsymbol{\mu}_{xy\{f,r\}}(t)\|dt
\end{aligned}$$

with $\{t, n\}$ referring to the tangential (t) and the normal (n) components, $\{f, r\}$ to the front (f) and rear (r) components, $\boldsymbol{\mu}_{xy}$ to the saturation of a tire in x and y directions, and T to the total simulation time. The tracking performance measures are evaluated for each benchmark problem.

B. Test Cases

All tests proposed by [5] are considered and run on each controller as benchmark problems. These include:

1) Initial Deviation: A small heading error (3°) and a lateral offset (0.2 m) are considered for the initial condition.

2) Low Road Adherence Coefficient: The road friction coefficient is reduced from 1.0 to 0.6. Tracking performances are evaluated for both cases in which this change is known or unknown to the controller.

3) Model Parameters Mismatch: Mass, rotational inertia, and the distance from the CG to the rear tire of the simulated vehicle are increased by 30%, while the controllers keep the old values.

4) Monte Carlo Simulations: The average performance under measurement errors is modeled by white Gaussian noise superimposed to the state that is used as feedback for the controller.

5) Worst-Case Disturbance using RRTs: Rapidly Exploring Random Trees (RRTs) can be used for general state space exploration. In our case, the algorithm used in [5] is employed for estimating the trajectory tracking worst-case performance under noisy vehicle state measurements. The RRT algorithm explores the state space of the system to search for the worst-case performance, i.e., the algorithm finds a sequence of measurement errors that maximizes the deviation with respect to the reference trajectory.

IV. Results

In this section we present the results of the selected test cases. The results of the first three tests (as numbered in Sec III-B) are shown for the double lane change scenario in Fig. 2. The tracking performance measures of these tests are summarized in Table II. We present the results of Monte Carlo simulations and RRTs for the single lane change scenario in Fig. 3 for investigating noise rejection properties.

A. Initial Deviation

For initial deviations, all methods have proven to be effective as shown in Fig. 2a. The FLAT, KINIO, and LQR controllers have an excellent convergence with low deviation, although the LQR introduces an overshoot. The BKST approach presents a large lateral overshoot and oscillations. The KINSM controller has relatively relaxed responses that cause the highest lateral deviations. I&I, HOSM, and PBPI have good convergence, although they all introduce a small overshoot and PBPI induces high longitudinal tracking error.

B. Low Road Adherence Coefficient

The tests investigating the control performance upon tire saturation are presented in Fig. 2b and Fig. 2c. These tests are the most revealing in terms of stability at the limit of controllability: kinematic-based controllers, as well as controllers that rely too much on the linear tire force assumption, do not provide reliable tracking. PBPI suffers heavily from this effect: the yaw dynamics is assumed to be asymptotically stable and therefore the controller does not actively compensate for the excessive yaw dynamics.

Controller FLAT performs best in this test due to the capability of fully compensating system dynamics (or at least up to the vehicle's physical limits). Interestingly, I&I has a similarly good performance, regardless of deviations of the road friction coefficient. The HOSM along with the BKST and LQR controller suffer from great deviations; nevertheless, they manage to keep the deviations contained.

C. Parameter Mismatch

The test on robustness towards parameter variation reveals a weakness of FLAT, KINIO, and KINSM, which only perform better than the PBPI due to a fixed offset with respect to the reference position as shown in Fig. 2d. While all model-based controllers are mostly affected in the tangential tracking, parameter variation increases the lateral tracking error of all controllers considerably.

D. Monte Carlo Simulation and Worst-Case Disturbance

The results of the Monte Carlo simulations and the worst-case analysis are presented in Fig. 3, where the dark trajectories correspond to Monte Carlo simulations, while the blue scatter plots represent the results of the RRTs. For both tests, 500 samples per time-step of 0.01s have been used as in [5]. The results of these tests reflect the noise robustness of each approach.

I&I, HOSM, and PBPI algorithms have a specific control action component designed to reject disturbances. However, out of these three controllers, only I&I reveals to be suitable against measurement noise as can be deducted by comparing the standard deviation plots of the position error as well as the maximum deviation plots in Fig. 4 and Fig. 5, respectively. Despite not having any particular method for noise suppression, the LQR performs better than any other controller in this test.

The difference in the worst-case performance of the controllers reveals that FLAT, KINIO, KINSM, PBPI, and HOSM

have large deviations and are therefore less robust in comparison to other techniques. I&I and LQR controllers produce very robust results in this test: the maximum deviations in the worst-case are close to the average cases.

E. Average-Error-Based Scoring

Table III presents relative, dimensionless error-based scores for each approach. The first column presents the number of free parameters for each controller, including the PD parameters when necessary. The remaining columns display the scores of the different algorithms for a certain category. The score is based on the combined average error vector $\boldsymbol{\varepsilon}_{comb}$, which contains the 2-norms of tangential and normal average deviations $\boldsymbol{\varepsilon}^{CG}_{avrg,\{t,n\}}$, as defined in subsection III-A and presented in Table II. Numbering the controllers with an index i from 1 to 8, the combined error for the i-th controller is the scalar quantity

$$\varepsilon_{comb,i} = \sqrt{\left(\varepsilon^{CG}_{avrg,t,i}\right)^2 + \left(\varepsilon^{CG}_{avrg,n,i}\right)^2}$$

and the combined error vector is

$$\boldsymbol{\varepsilon}_{comb} = \left[\varepsilon_{comb,1}, \cdots, \varepsilon_{comb,8}\right].$$

The score s_i of the i-th controller is calculated as:

$$s_i = \frac{\varepsilon_{comb,i}}{\min(\boldsymbol{\varepsilon}_{comb})},$$

where the $\min(\boldsymbol{a})$ operator picks the smallest element from vector $\boldsymbol{a}$. In this manner, for each category, the best controller receives a score of 1, and the others express their score in error-units normalized by the best result.

F. Remark

The tuning phase of the controllers is particularly crucial for a meaningful comparison since the outcomes of the simulations can be influenced significantly by different gains. However, while even limited variations on the gains certainly impact the tracking precision, it has been noticed that most of the controller properties (e.g., stability, noise rejection, robustness to model variations) are not strongly compromised. Although the conclusions drawn from the obtained results might not be absolute, they are helpful when deciding which controllers to consider.

V. Conclusion

Using the framework from [5], we provide an extensive comparison of eight different state-of-the-art control methods. For the first time, a wide variety of controllers is tested and compared while taking extreme situations and real-world effects such as disturbances, noise, and parameter mismatch into account. Since the considered controllers are representatives of different general controller families, this work offers a starting point when choosing the appropriate controller for a given control task. Depending on the constraints and specific demands, one can use the results to select the control scheme which is best suited for the task without having to implement and test a wide variety of controllers each time. Since we have a transparent and standardized comparison, the evaluation of the controllers is as fair as currently possible.

Measurement Noise Robustness: Compared to all other approaches, I&I and LQR strategies are found to be more robust against measurement noise.

Kinematic-based Approaches: It has emerged that kinematic-based controllers (KINIO and KINSM) are unsuitable in situations where the tire forces reach saturation because they cause large lateral deviations from the reference trajectory. They do not suffer, however, from bad conditioning when the vehicle speed reaches zero. As a consequence, these methods are still useful for parking or low-speed driving applications.

Sliding Mode: Sliding mode controllers are useful for compensating model errors. However, by design, sliding mode control actions can be aggressive: tracking performances are greatly degraded due to the rapid changes of the sliding control input which quickly causes saturation of the tire forces.

Linear Tire Model-based Controllers: Controllers that are based on the linear tire model (HOSM, PBPI, I&I, BKST, and LQR) perform satisfactorily on most of the tests, but their performance degrades considerably for low road adherence conditions. These controllers find good application in the case of normal highway driving. An interesting result is obtained by the I&I controller: despite a simple control law and a light weight implementation, this controller performs above average in every test.

Flatness-based Control: Flatness-based control of the vehicle (tire force inversion based strategy from [5]) gives the overall best results in terms of precision and stability in case of low adherence of the tires. Since FLAT is derived from the model utilized in simulation, its very good performance in almost every test may be sightly biased. Due to the model-inversion algorithm, this controller is certainly superior to any other hereby presented technique in compensating model dynamics. However, FLAT does show some weaknesses. As Monte Carlo Simulations and RRTs have revealed, this algorithm has limited noise suppression capabilities. Additionally, the controller is quite sensitive to model parameters: a separate adaptive control scheme could solve this problem by adjusting the parameters online.

References

[1] G. Tagne, R. Talj, and A. Charara, "Higher-order sliding mode control for lateral dynamics of autonomous vehicles, with experimental validation," in *Intelligent Vehicles Symposium (IV)*. IEEE, 2013, pp. 678–683.

[2] M. Manceur and L. Menhour, "Higher order sliding mode controller for driving steering vehicle wheels: Tracking trajectory problem," in *52nd Annual Conference on Decision and Control (CDC)*. IEEE, 2013, pp. 3073–3078.

[3] R. Solea and U. Nunes, "Trajectory planning and sliding-mode control based trajectory-tracking for cybercars," *Integr. Comput.-Aided Eng.*, vol. 14, no. 1, pp. 33–47, 2007.

[4] S. C. Peters, E. Frazzoli, and K. Iagnemma, "Differential flatness of a front-steered vehicle with tire force control," in *International Conference on Intelligent Robots and Systems (IROS)*. IEEE, 2011, pp. 298–304.

[5] D. Heß, M. Althoff, and T. Sattel, "Comparison of trajectory tracking controllers for emergency situations," in *Intelligent Vehicles Symposium (IV)*. IEEE, 2013, pp. 163–170.

[6] D. Kim, J. Kang, and K. Yi, "Control strategy for high-speed autonomous driving in structured road," in *14th International IEEE Conference on Intelligent Transportation Systems (ITSC)*, 2011, pp. 186–191.

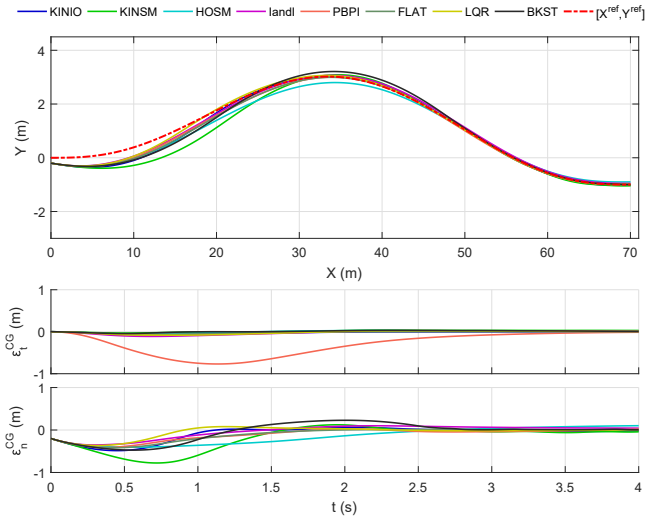

(a) Test 1: Initial deviation

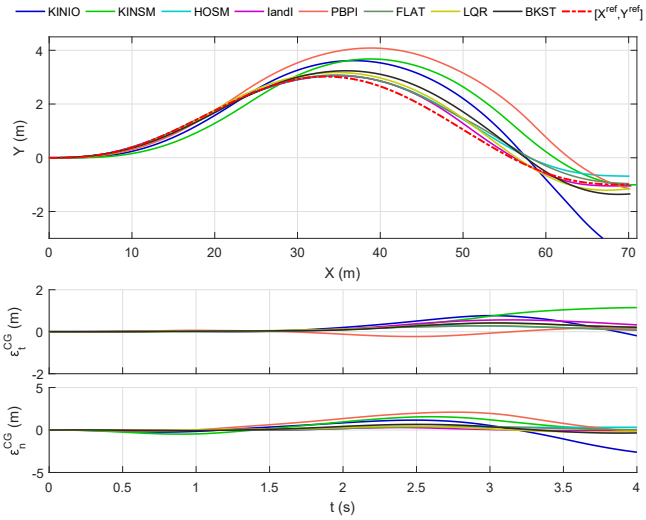

(b) Test 2a: Low road friction coefficient

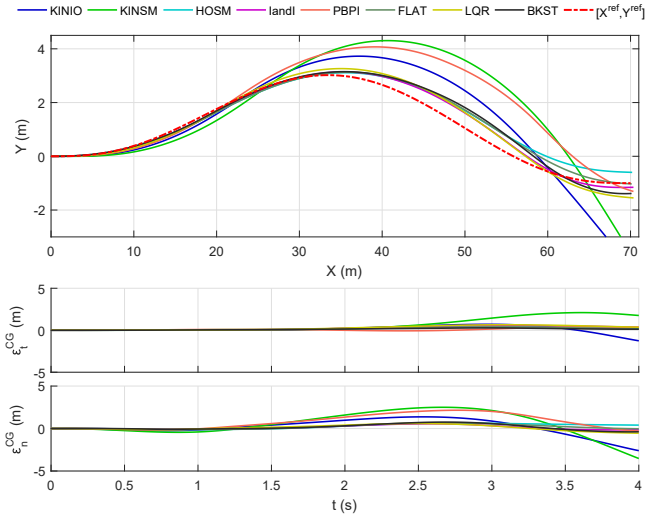

(c) Test 2b: Unknown low road friction coefficient

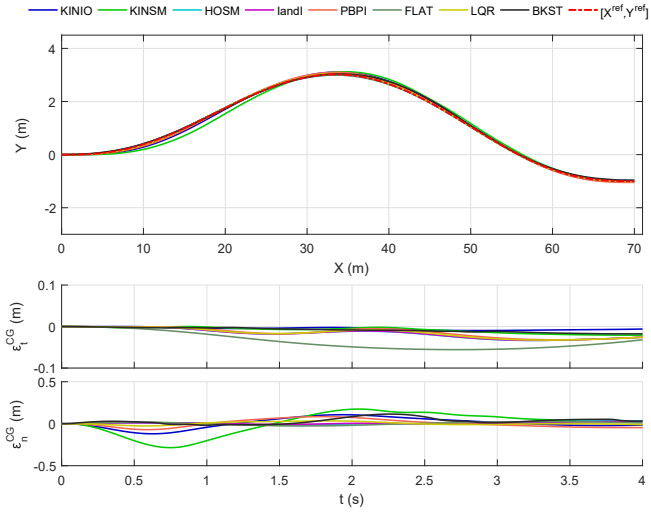

(d) Test 3: Mismatched parameters (m, J, l_R)

Fig. 2. Resulting system trajectories for tests 1-3

[7] J. Guo, P. Hu, and R. Wang, "Nonlinear coordinated steering and braking control of vision-based autonomous vehicles in emergency obstacle avoidance," *IEEE Trans. Intell. Transport. Syst.*, pp. 1–11, 2016.

[8] M. Werling, L. Groll, and G. Bretthauer, "Invariant trajectory tracking with a full-size autonomous road vehicle," *IEEE Transactions on Robotics*, vol. 26, no. 4, pp. 758–765, 2010.

[9] S. Hima, S. Glaser, A. Chaibet, and B. Vanholme, "Controller design for trajectory tracking of autonomous passenger vehicles," in *14th International IEEE Conference on Intelligent Transportation Systems (ITSC)*, 2011, pp. 1459–1464.

[10] R. Sharp, "Application of linear optimal preview control theory to severe braking of a car," *Proceedings of the Institution of Mechanical Engineers, Part C: Journal of Mechanical Engineering Science*, vol. 225, no. 5, pp. 1097–1106, 2011.

[11] R. Attia, R. Orjuela, and M. Basset, "Combined longitudinal and lateral control for automated vehicle guidance," *Vehicle System Dynamics*, vol. 52, no. 2, pp. 261–279, 2014.

[12] V. Turri, A. Carvalho, H. E. Tseng, K. H. Johansson, and F. Borrelli, "Linear model predictive control for lane keeping and obstacle avoidance on low curvature roads," in *16th International IEEE Conference on Intelligent Transportation Systems (ITSC)*, 2013, pp. 378–383.

[13] S. Chaib, M. S. Netto, and S. Mammar, "H_∞, adaptive, PID and fuzzy control: a comparison of controllers for vehicle lane keeping," in *Intelligent Vehicles Symposium*. IEEE, 2004, pp. 139–144.

[14] G. Tagne, R. Talj, and A. Charara, "Design and comparison of robust nonlinear controllers for the lateral dynamics of intelligent vehicles," *IEEE Transactions on Intelligent Transportation Systems*, vol. 17, no. 3, pp. 796–809, 2016.

[15] D. Cole, A. Pick, and A. Odhams, "Predictive and linear quadratic methods for potential application to modelling driver steering control," *Vehicle System Dynamics*, vol. 44, no. 3, pp. 259–284, 2006.

[16] D. Soudbakhsh and A. Eskandarian, "Comparison of linear and nonlinear controllers for active steering of vehicles in evasive manoeuvres," *Proceedings of the institution of mechanical engineers, part I: Journal of Systems and Control Engineering*, vol. 226, no. 2, pp. 215–232, 2012.

[17] S. Dominguez, A. Ali, G. Garcia, and P. Martinet, "Comparison of lateral controllers for autonomous vehicle: Experimental results," in *19th International Conference on Intelligent Transportation Systems (ITSC)*. IEEE, 2016, pp. 1418–1423.

[18] B. Siciliano, L. Sciavicco, L. Villani, and G. Oriolo, *Robotics*. Springer

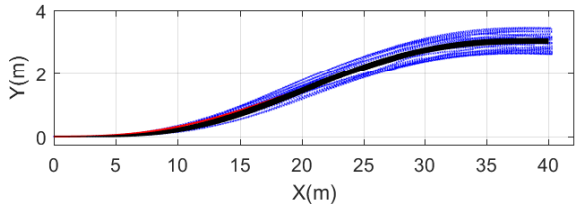

(a) KINIO

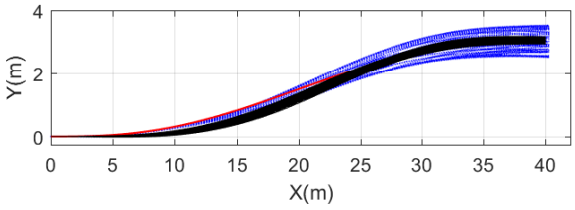

(b) KINSM

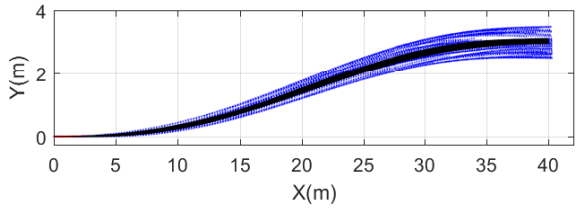

(c) HOSM

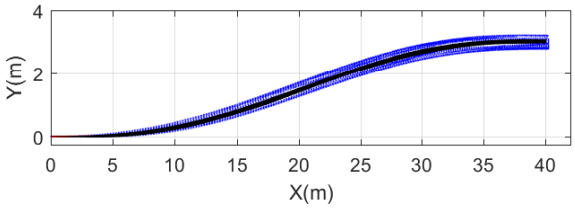

(d) I&I

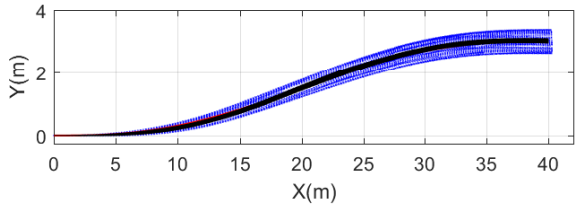

(e) PBPI

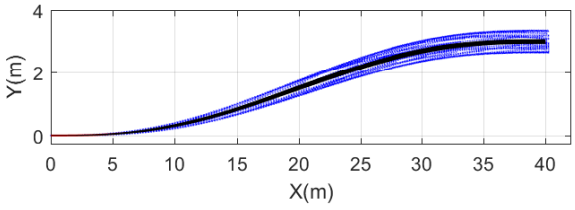

(f) FLAT

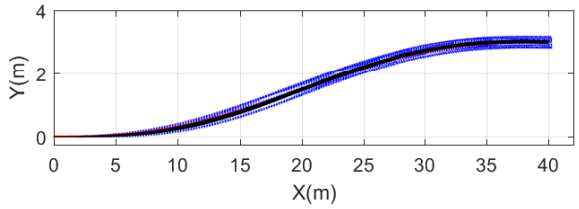

(g) LQR

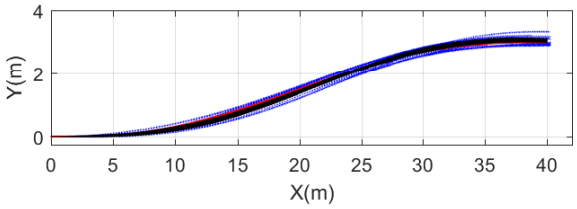

(h) BKST

Fig. 3. Monte-Carlo and RRT analysis. The dark trajectories correspond to Monte Carlo simulation, the blue scatter plots to the results of the RRTs

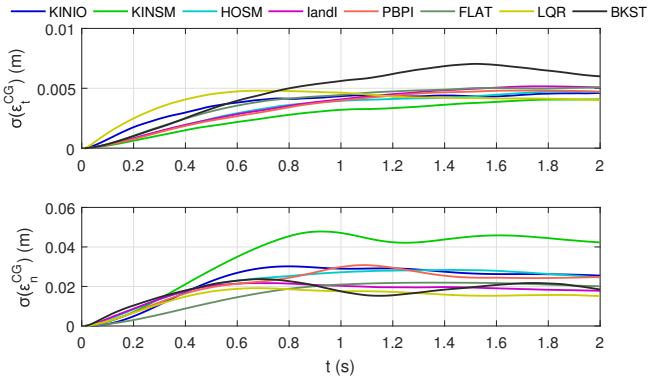

Fig. 4. Test 4: Standard deviation of error using Monte Carlo simulation

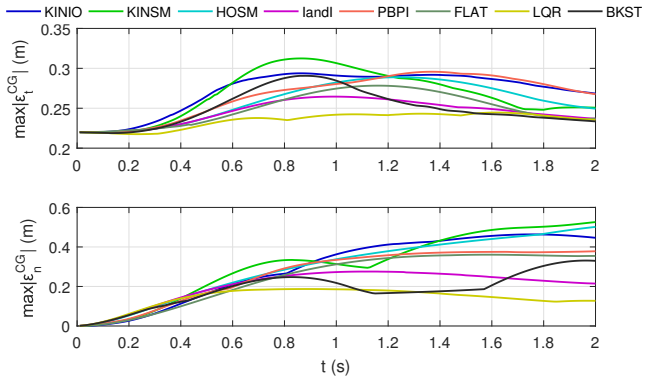

Fig. 5. Test 5: Maximum error using RRTs

London, 2009.

[19] J. M. Snider, "Automatic steering methods for autonomous automobile path tracking," *Robotics Institute, Pittsburgh, PA, Tech. Rep. CMU-RITR-09-08*, 2009.

TABLE II
RESULTS OF THE DOUBLE LANE CHANGE SCENARIO

	max. deviation (m)		**avrg. deviation (m)**		**final deviation (m)**		**avrg. tire saturation**	
	tangential	normal	tangential	normal	tangential	normal	tangential	normal
1) Initial Deviation								
KINIO	7.37e-02	4.85e-01	2.20e-02	1.08e-01	-3.90e-04	-1.68e-02	0.54	0.45
KINSM	3.66e-02	7.76e-01	2.32e-02	2.14e-01	3.01e-02	-4.22e-02	0.57	0.45
HOSM	5.73e-02	4.04e-01	2.17e-02	1.88e-01	7.88e-03	1.02e-01	0.50	0.36
I&I	1.12e-01	3.51e-01	3.81e-02	1.15e-01	9.64e-03	4.41e-02	0.52	0.39
PBPI	7.68e-01	4.13e-01	2.99e-01	1.11e-01	-1.26e-02	1.66e-02	0.50	0.39
FLAT	6.13e-02	4.19e-01	1.70e-02	1.06e-01	1.62e-04	3.28e-04	0.51	0.39
LQR	8.29e-02	3.65e-01	3.14e-02	7.77e-02	9.21e-03	1.09e-02	0.53	0.42
BKST	4.35e-02	4.74e-01	1.93e-02	1.62e-01	6.96e-03	6.32e-03	0.60	0.44
2a) Tire Force Saturation, μ_0 = 0.6 known								
KINIO	7.66e-01	2.61e+00	2.53e-01	6.66e-01	-1.93e-01	-2.61e+00	0.91	0.89
KINSM	1.15e+00	1.56e+00	3.59e-01	6.15e-01	1.15e+00	1.55e-03	0.88	0.78
HOSM	2.86e-01	3.75e-01	1.20e-01	1.75e-01	1.07e-01	3.15e-01	0.80	0.57
I&I	5.63e-01	2.96e-01	2.28e-01	7.74e-02	3.26e-01	-4.58e-02	0.84	0.64
PBPI	2.29e-01	2.10e+00	8.96e-02	8.57e-01	1.54e-01	-1.54e-01	0.91	0.78
FLAT	2.80e-01	4.62e-01	1.07e-01	1.49e-01	6.79e-02	3.62e-02	0.82	0.59
LQR	4.01e-01	4.49e-01	1.67e-01	1.65e-01	2.12e-01	-1.52e-01	0.86	0.69
BKST	4.18e-01	6.61e-01	1.61e-01	2.46e-01	2.11e-01	-3.45e-01	0.89	0.63
2b) Tire Force Saturation, μ_0 = 0.6 unknown								
KINIO	1.26e+00	2.61e+00	2.78e-01	7.02e-01	-1.26e+00	-2.61e+00	0.92	0.90
KINSM	2.10e+00	3.53e+00	6.76e-01	1.15e+00	1.76e+00	-3.53e+00	0.87	0.87
HOSM	4.00e-01	6.49e-01	1.86e-01	3.01e-01	1.99e-01	4.02e-01	0.80	0.55
I&I	5.62e-01	5.53e-01	2.53e-01	1.87e-01	3.54e-01	-1.54e-01	0.84	0.63
PBPI	3.98e-01	2.15e+00	1.20e-01	8.70e-01	3.54e-01	-3.08e-01	0.91	0.77
FLAT	3.99e-01	6.68e-01	1.69e-01	2.46e-01	1.45e-01	-2.81e-02	0.81	0.56
LQR	6.52e-01	5.89e-01	2.88e-01	2.56e-01	3.64e-01	-5.49e-01	0.85	0.66
BKST	2.79e-01	7.58e-01	1.27e-01	2.56e-01	1.25e-01	-3.84e-01	0.89	0.64
3) Mismatched Parameters								
KINIO	9.60e-03	1.20e-01	5.01e-03	5.08e-02	-6.02e-03	-1.56e-02	0.46	0.35
KINSM	2.08e-02	2.85e-01	8.23e-03	1.08e-01	-2.07e-02	3.06e-02	0.48	0.37
HOSM	3.35e-02	3.57e-02	1.68e-02	1.15e-02	-2.58e-02	3.27e-02	0.45	0.33
I&I	3.33e-02	2.72e-02	1.66e-02	8.33e-03	-2.58e-02	2.52e-02	0.45	0.33
PBPI	3.19e-02	8.41e-02	1.44e-02	3.91e-02	-2.52e-02	-4.58e-02	0.46	0.35
FLAT	5.56e-02	2.66e-02	3.52e-02	1.53e-02	-3.19e-02	8.73e-03	0.44	0.32
LQR	3.25e-02	3.31e-02	1.56e-02	1.32e-02	-2.57e-02	-1.04e-02	0.45	0.34
BKST	1.76e-02	1.15e-01	8.29e-03	3.63e-02	-1.76e-02	2.99e-02	0.51	0.35

TABLE III
SCORES

Controller	**Number of Free Parameters**	**Precision (Nominal Case)**	**Robustness to Parametric Uncertainties**	**Handling at Physical Limits**	**Robustness to Measurement Noise**
KINIO	3	1.15e+03	2.75	3.88	1.78
KINSM	7	2.88e+03	5.84	3.87	1.99
HOSM	5	0.59e+03	1.09	1.15	1.88
I&I	5	0.44e+03	1.00	1.31	1.24
PBPI	7	1.11e+03	2.24	4.69	1.56
FLAT	3	1.00	2.07	1.00	1.48
LQR	5	0.61e+03	1.10	1.28	1.00
BKST	10	0.64e+03	2.00	1.60	1.43